Journal of Magnetism and Magnetic Materials 350 (2014) 119–123

Contents lists available at ScienceDirect

Journal of Magnetism and Magnetic Materials

journal homepage: www.elsevier.com/locate/jmmm

# First-principle prediction of robust half-metallic Te-based half-Heusler alloys

Shi-Yuan Lin [a], Xiao-Bao Yang [a], Yu-Jun Zhao [a,b,*]

[a] Department of Physics, South China University of Technology, Guangzhou 510640, China
[b] State Key Laboratory of Luminescent Materials and Devices, South China University of Technology, Guangzhou 510640, China

ARTICLE INFO

*Article history:*
Received 4 June 2013
Received in revised form
20 August 2013
Available online 25 September 2013

*Keywords:*
First-principle calculation
Half-Heusler alloy
Half-metal

ABSTRACT

Te-based half-Heusler systems are studied by first-principle calculations to search for alloys with stable half-metallic properties. We found that CoMnTe and FeMnTe are the most robust half-metallic (HM) ferromagnetic alloys among the 90 studied alloys, with HM gaps of 0.42 and 0.61 eV, respectively, larger than that of any Heusler or half-Heusler alloys reported in the literature. The half-metallicity of CoMnTe and FeMnTe is found to be robust under large in-plane strains, which makes them suitable for practical spintronic device applications.



## 1. Introduction

Half-metallic (HM) ferromagnets have attracted much interest in the past decades since their 100% spin polarized states at the Fermi level hold great promise for applications in spintronics [1]. So far HM property has been reported in magnetic oxides [2–5], double perovskite [6], rare-earth nitrides [7,8], zinc-blende transition metal pnictides [9–11], chalcogenides [12], and Heusler alloys [13–20]. The HM Heusler alloys have relatively high Curie temperature [21,22] compared with other HM systems, and their structures match well with zinc-blende structure (including the similar diamond structure), which dominates the semiconductors electronic industry.

In addition to the stability of ferromagnetism, the magnitude of the HM gap (the energy difference between the highest occupied spin-up and spin-down states) is crucial for the application of half-metal Heusler alloys, since it affects the performance of spin injection devices. Unfortunately, most of the reported HM half-Heusler alloys have small HM gaps. For instance, the first-principles calculations predicted HM gaps for FeMnSb [23], NiCrP [24], NiCrSe [24], NiCrTe [24], and NiVAs [25] are only 0.2, 0.263, 0.047, 0.102, and 0.07 eV, respectively. The small HM gaps would often disappear in these half-Heusler alloys when strains from mismatch exist in their interface with conventional semiconductors. Therefore, exploring new HM materials with large HM gaps is crucial for practical spintronic device applications, although half-Heusler alloys CoCrP and CoCrAs were predicted to be HM ferromagnetic alloys with much larger HM gaps (~0.5 eV) recently [26].

In this work, we performed systematic search of the Te-based half-Heusler alloys through first-principles calculations, and found that CoMnTe and FeMnTe are robust HM alloys with large HM gaps of 0.42 and 0.61 eV and band gaps in minority spin channel of 1.13 and 1.24 eV, respectively. The half-metallicity of CoMnTe and FeMnTe can be maintained even under in-plane strains of −11.3% to 6.1% and −11.7% to 10.0%, respectively.

The calculations were carried out with the spin polarized density functional theory (DFT) as implemented in Vienna *ab initio* simulation package (VASP) [27]. The generalized gradient approximation (GGA) of PBE [28] was adopted for the exchange and correlation functional. A plane wave cutoff of 450 eV and a $5\times5\times5$ Monkhorst–Pack $k$-point mesh are used for the calculation. The total energy and eigenvalues are converged to be within 10 meV and the HM band gap changes within 3 meV with respect to the $k$-points according to the test calculations with a $k$ mesh of $9\times9\times9$ for most of the alloys with HM gaps of $>0.2$ eV, including CoVTe, FeVTe, CoCrTe, FeCrTe, CoMnTe, and FeMnTe. We also considered the site preference of X and Y atoms in XYTe. We found that the atoms with larger number of valence electrons prefer X site for most of the systems, except NiCoTe, Cu based and Zn based systems. In particular, most of the interesting alloys with HM gaps larger than 0.2 eV, including CoVTe, FeVTe, CoCrTe, FeCrTe, CoMnTe and FeMnTe, obey the valence electron rule and their energy differences for site preference are more than 500 meV/atom in general. This means that these large gap half-metal systems are rather robust with respect to site preference. Nevertheless, we will discuss all the possible half-metallic properties of XYTe with both X and Y from Sc to Zn. For the calculations

* Corresponding author at: South China University of Technology, Department of Physics, 381 Wushan Road, Guangzhou 510640, China. Tel.: +86 20 87110426; fax: +86 20 87112837.
*E-mail address:* zhaoyj@scut.edu.cn (Y.-J. Zhao).

0304-8853/$ - see front matter © 2013 Elsevier B.V. All rights reserved.
http://dx.doi.org/10.1016/j.jmmm.2013.09.026

of local magnetic moments and projected density of states, the default PAW radii from VASP code are used. To confirm the reliability of our calculation, we also calculated the HM gaps of CoCrP and CoCrAs. The calculated HM gaps are 0.42 and 0.51 eV, correspondingly, which are in excellent agreement with the FLAPW values obtained by Yao et al. [26] (0.46 and 0.51 eV, respectively).

## 2. XYTe half-Heusler alloys

The crystal structure of half-Heusler compounds is described by the space group $F\bar{4}3m$ with $C1_b$ structure and the atomic arrangement is presented in Fig. 1. The positions of the basis atoms in Wyckoff coordinates are as follows: X atoms at (0 0 0), Y atoms at (1/4 1/4 1/4) and Te atoms at (3/4 3/4 3/4), in analogy with filled tetrahedral compounds [29].

In order to explore systems with larger HM gaps, various Te-based half-Heusler alloys XYTe (X=Sc–Zn, and Y=Sc–Zn) are investigated. It was reported that some Mn containing half-Heusler compounds may not be stable in contrast to other structures. For instance, CoMnSb crystallizes in a cubic superstructure, which can be illustrated by alternating MnSb and $Co_2MnSb$ cells [30]. These half-Heusler compounds, however, may be still stabilized by strains, which are hard to avoid in the interface of devices. The strain effect on the HM properties will be addressed later. Here, we consider the stability of ferromagnetic (FM) and antiferromagnetic (AFM) phases in a 12-atom unit cell. Of note, here AFM and FM configurations refer to the spin arrangement of element Y in XYTe since Y contributes the most to magnetic moments. In detail, half of the Y atoms in a tetrahedron were aligned antiparallel to the other half. We found that 49 alloys of the studied 90 candidates are in favor of FM phases. Most of the alloys with FM phases are in the region of X=V–Co, but only a few of them follow the Slater–Pauling rule [31] with integral total magnetic moment. On the other hand, 41 alloys are in AFM configurations which correspond to alloys of X=Ni–Zn, or X=Sc–Ti, except Y=Mn–Co. For instance, CuCrTe favors an AFM configuration, with the local magnetic moments of Cr atoms around 4.07 $\mu_B$. We also found that most of the alloys with FM phases contain atoms with large magnetic moment, such as Cr, Mn, and Fe, while the AFM alloys often contain atoms with negligible local moment, such as Sc, Cu, and Zn.

All the calculated band gaps and HM gaps are shown in Fig. 2 for Te-based half-Heusler alloys XYTe (X=Sc–Zn, and Y=Sc–Zn with $X \neq Y$). It is clear that the systems with large band-gap are mostly in the middle region, which corresponds to X=Cr–Co, Y=Ti–Mn. Clearly the HM gaps are much smaller, with only a few alloys having relatively large HM gaps, which correspond to alloys of X=Fe or Co, Y=V–Mn.

In Table 1, we list the calculated equilibrium lattice constant, energy difference between the AFM and FM phases, minority spin channel band gap, and HM gap for most of the alloys with HM gaps larger than 0.2 eV, including CoVTe, FeVTe, CoCrTe, FeCrTe, CoMnTe, and FeMnTe. It is clear that their FM phases are rather stable with respect to the corresponding AFM phases. In particular, the exchange energies for CoCrTe, FeCrTe, CoMnTe, and FeMnTe are all greater than 100 meV/formula. We found that the HM gap of FeMnTe is as large as 0.61 eV, larger than any reported HM gaps for Heusler or half-Heusler alloys in the literature. Its corresponding band gap in minority spin channel reaches 1.24 eV, indicating that the Fermi level is pinned nearly at the mid-gap to maximize the HM gap. In the

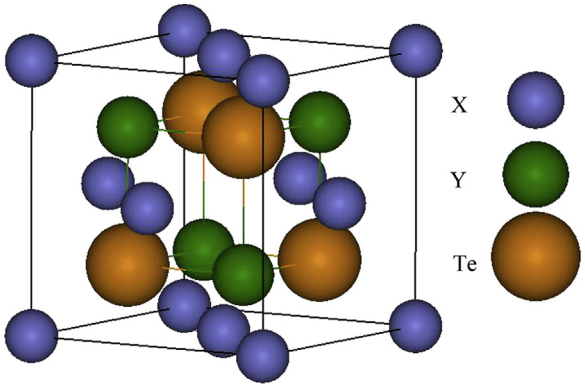


**Fig. 1.** The crystal structure of half-Heusler compounds XYTe.

**Table 1**
Calculated equilibrium lattice constant ($a_0$), energy difference between the antiferromagnetic and ferromagnetic phases ($\Delta E$), band gap ($E_g$), and HM gap ($E_g^{HM}$) of the HM half-Heusler alloys XYTe. Here, AFM and FM configurations refer to the spin arrangement of element Y in XYTe.

| Compound | $a_0$ (Å) | $\Delta E$ (eV/formula) | $E_g$ (eV) | $E_g^{HM}$ (eV) |
|---|---|---|---|---|
| CoVTe | 5.88 | 0.09 | 1.05 | 0.21 |
| FeVTe | 5.82 | 0.06 | 1.31 | 0.20 |
| CoCrTe | 5.87 | 0.12 | 0.78 | 0.27 |
| FeCrTe | 5.87 | 0.13 | 0.91 | 0.34 |
| CoMnTe | 5.86 | 0.17 | 1.13 | 0.42 |
| FeMnTe | 5.84 | 0.12 | 1.24 | 0.61 |

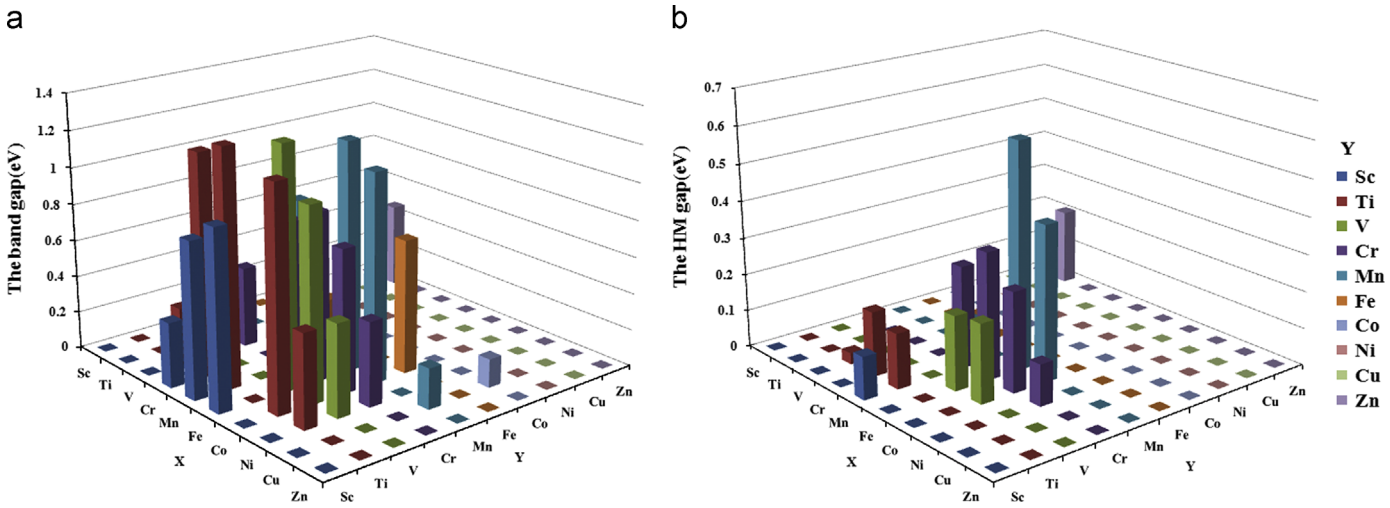


**Fig. 2.** The band gaps (a) of minority spin channel and corresponding HM gaps (b) of Te-based half-Heusler XYTe alloys.

following, we will pay more attention to CoMnTe and FeMnTe alloys due to their largest HM gaps in the studied alloys.

The calculated local magnetic moments and total magnetic moments of CoMnTe and FeMnTe are listed in Table 2, along with the other half-Heusler alloys with HM gaps larger than 0.2 eV. We found that the total magnetic moments of the studied systems obey the rule for HM half-Heusler alloys mentioned earlier [31]: $M_t = Z_t - 18$, where $M_t$ stands for the total magnetic moment (in $\mu_B$) per formula unit and $Z_t$ represents the total number of valence electrons. The local magnetic moments of Co, Mn, and Te atoms of CoMnTe are, respectively, 0.384, 3.501, and $-0.035\ \mu_B$, and those of Fe, Mn, and Te atoms of FeMnTe are $-0.409$, 3.276 and $-0.009\ \mu_B$. In FeYTe (Y=V, Cr, and Mn) half-Heusler alloys, the calculated local magnetic moments of Fe atom are orientated along the minority spin direction. This can be explained by the spin-dependent partial density of states (DOS) of the systems, which are exemplified by CoMnTe and FeMnTe in Fig. 3. The magnetic moment is mainly contributed from the transition metals with a smaller atomic number (Mn atom here), since their d levels are relatively higher in energy, and thus dominates the antibonding states, leading to a high spin configuration. The negative moment of Fe atom could appear when its contribution to the antibonding states in minority spin channel is small (i.e., close to a full occupation in minority channel as shown in Fig. 3) and its majority 3d levels are not fully occupied.

**Table 2**
Calculated local magnetic moments and total magnetic moments of XYTe alloys with large HM gaps.

| Compound | Local magnetic moment ($\mu_B$) | | | Total ($\mu_B$) |
|---|---|---|---|---|
| | X | Y | Te | |
| CoVTe | 0.10 | 1.83 | −0.03 | 2.00 |
| FeVTe | −0.56 | 1.49 | −0.01 | 1.00 |
| CoCrTe | −0.27 | 3.17 | −0.06 | 3.00 |
| FeCrTe | −1.11 | 2.96 | −0.01 | 2.00 |
| CoMnTe | 0.38 | 3.50 | −0.04 | 4.00 |
| FeMnTe | −0.41 | 3.28 | −0.01 | 3.00 |

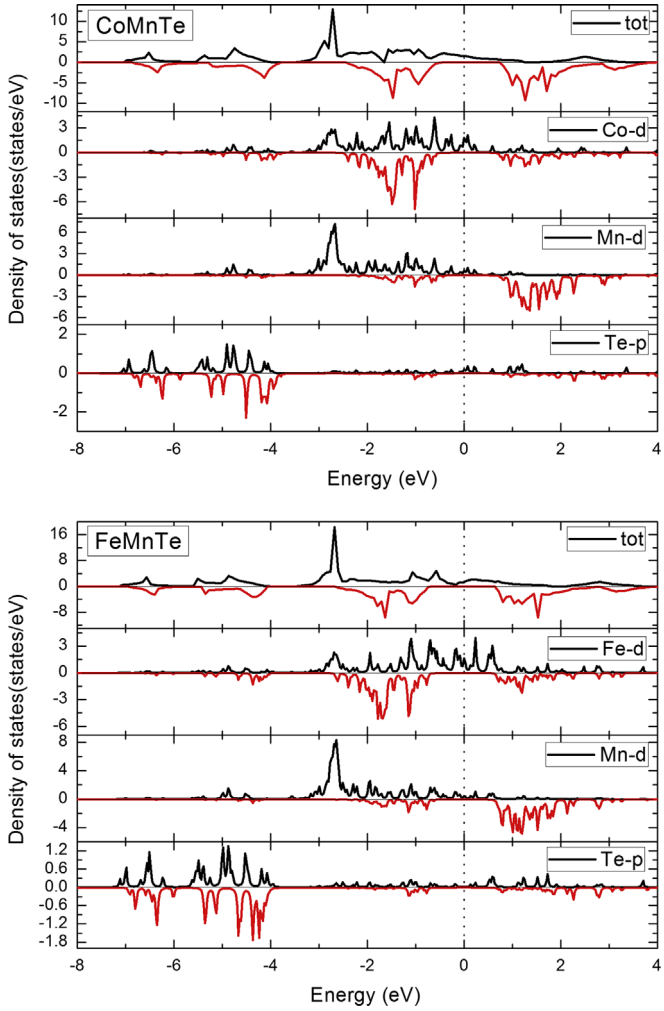


**Fig. 3.** The spin-dependent total (tot) and partial DOSs of CoMnTe (upper panel) and FeMnTe (lower panel). The Fermi level is set to zero and indicated by the dotted line.

From Fig. 3, it is clear that the s and p levels of the Te ions are hybridized with d levels of Mn and Co/Fe in CoMnTe/FeMnTe. In the majority-spin component, Mn 3d states are mostly occupied and hybridized with Co 3d or Fe 3d states. In the minority-spin component, most unoccupied Mn 3d states are found between 1.0 and 2.0 eV above $E_F$. The Co 3d or Fe 3d levels are hybridized with Mn 3d levels, with their bonding and antibonding levels dominating the valence band and conduction band, respectively. The band gap can be regarded to be originating from the strong d–d hybridization between the two transition metal ions. We also found from the spin-dependent band structures calculation that in the minority spin channel of CoMnTe and FeMnTe, the valence band maximum (VBM) is at Γ-point while the conduction band minimum (CBM) is at X-point, implying that the band gaps of both alloys are indirect. The calculated band gaps are, correspondingly, 1.13 and 1.24 eV, which are clearly larger than those of NiCrP, NiCrSe and NiCrTe [24]. It is known that spin–orbit coupling (SOC) can mix the spin-up and spin-down states, thus destroying the band gap. To check this, we have conducted a test calculation on FeMnTe with and without SOC using the full-potential linearized-muffin-tin-orbital (LMTO) method [32]. We found that the SOC effect does not introduce significant states in the band gap on the spin minority channel, in line with the results on HM NiMnSb, reported by Lezaic et al. [33]; thus, for practical application, the SOC effect can be neglected.

## 3. Stability of HM property of CoMnTe and FeMnTe

It is worthwhile to further investigate the strain effect on the stability of half-metallicity for CoMnTe and FeMnTe. In practice, an in-plane strain, rather than a uniform strain, should be considered for the stability of HM properties of the half-Heusler materials, since the strains often come from the interface in potential applications. Firstly we checked the stability of their ferromagnetism by calculating the total energy of CoMnTe and FeMnTe as a function of the lattice constant $a$ for the FM and AFM phases under a biaxial strain (as shown in Fig. 4). In the calculations, the $c$-axis is unconstrained (free to relax) for a given in-plane lattice constant $a$. The ground energy after the distortion is higher than that of the cubic cell as expected. It is true that the cubic half-Heusler structure could be unstable since very few experimental reports are available. This should result from the comparison of its stability to those of some possible competing phases under thermal equilibrium condition. Nevertheless, the thin film of the cubic half-Heusler structure could be realized by a nonequilibrium method (e.g. MBE). This is why we investigate the strain effect on the stability of half-metallicity for CoMnTe and FeMnTe. Also we found that the FM phase is energetically favored for both CoMnTe and FeMnTe in the range of studied lattice constants from 5.55 Å to 6.15 Å. This implies that there is no magnetic phase transition when a wide range of strains are applied.

In order to study the stability of the half metallicity in response to the in-plane strains, we then calculated the gaps of CoMnTe and

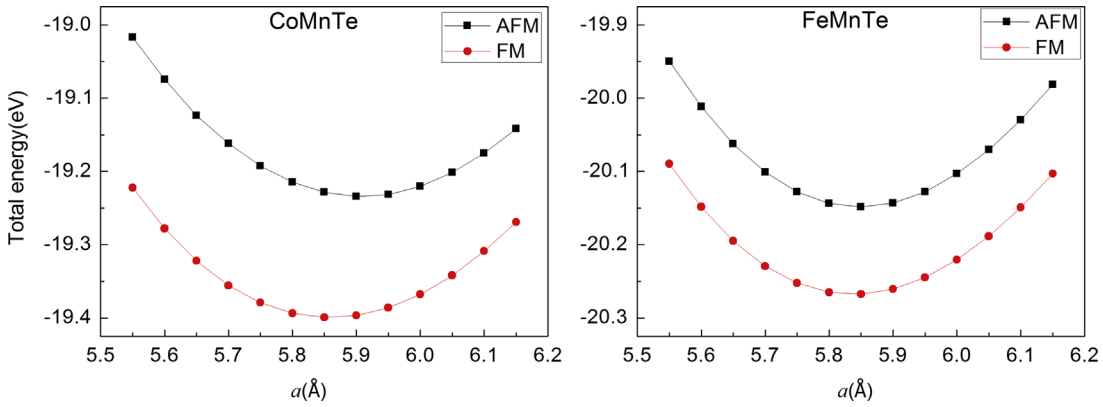


**Fig. 4.** Total energies of ferromagnetic and antiferromagnetic phases as a function of the in-plane lattice constant for CoMnTe and FeMnTe.

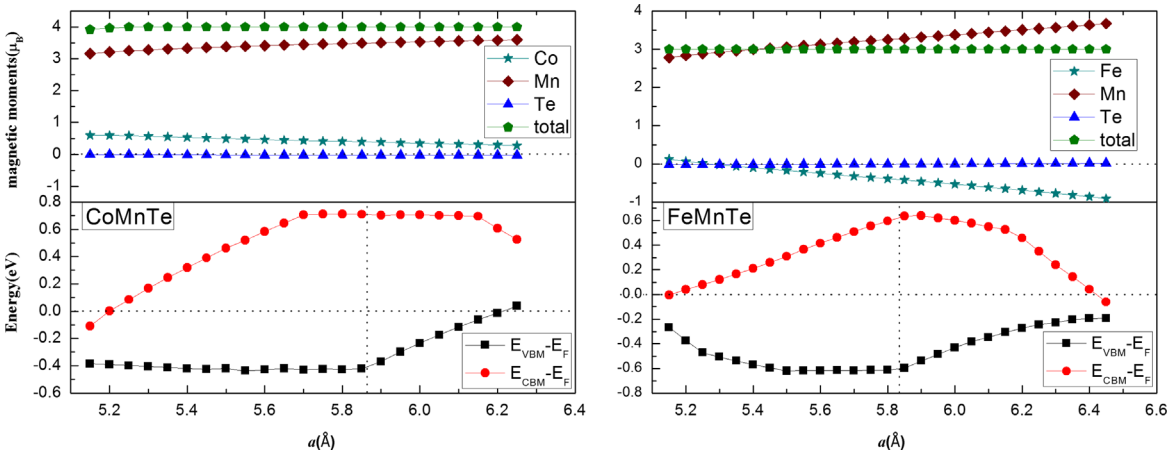


**Fig. 5.** Calculated $E_{VBM}-E_F$ (black squares) and $E_{CBM}-E_F$ (red dots, corresponding to HM gap) values in the minority-spin channel, as well as the total and local magnetic moments of CoMnTe and FeMnTe at various in-plane lattice constants. The Fermi level is set to zero and indicated by the horizontal dotted line; the vertical dotted line indicates the equilibrium lattice. (For interpretation of the references to color in this figure legend, the reader is referred to the web version of this article.)

FeMnTe in minority spin channel as a function of in-plane lattice constant that changes in the range 5.15–6.25 Å and 5.15–6.45 Å, i.e. with a strain of −12.2% to 6.6% and −11.7% to 10.5%, respectively. The energy difference from VBM to the Fermi level and from CBM to the Fermi level in the minority-spin channel of CoMnTe and FeMnTe is shown in Fig. 5. We noticed that both the band gaps (corresponding to the energy difference between the red and black points in Fig. 5) and HM gaps decrease rapidly when the lattice constant increases from the equilibrium value, while the change is much slower under negative strains. The alloys lose their HM property and become metallic when the Fermi level is out of the gap. Therefore, CoMnTe and FeMnTe retain HM property at the in-plane lattice constants between 5.20 Å and 6.22 Å and between 5.15 Å and 6.42 Å, respectively. That is, CoMnTe and FeMnTe can maintain their half-metallicity with the biaxial strain in the range of −11.3% to 6.1% and −11.7% to 10.0% with respect to their equilibrium lattice constants, respectively.

In addition, we checked the robustness of the half metallicity of CoMnTe and FeMnTe in response to the uniform strain (i.e. corresponding to hydrostatic pressure), and found that they retain HM property with lattice constant changes in the range of −8.2% to 6.3% and −7.8% to 6.0%. This is clearly more robust than that of NiMnSb (−2% to 3%) [34]. Our result suggests that CoMnTe and FeMnTe can maintain their half-metallicity under a strong biaxial strain during epitaxial growth of films. Therefore, the two alloys show great promise in the applications of spin valve and magnetic tunnel junction. The total and local magnetic moments of CoMnTe and FeMnTe as a function of the in-plane lattice constants are also shown in Fig. 5. We noticed that the tensile strain leads to an increasing local magnetic moment of Mn ions, while the local magnetic moment of Co or Fe ions gets smaller and finally even changes its orientation. The increase of local Mn moments is due to the decreasing overlap of wave functions as the lattice expands [35]. To compensate this increase, the magnetic moments of Fe ion change their sign, transforming the magnetic structure from ferromagnetic to ferrimagnetic [36].

Finally, we have studied the trend of gaps of CoMnZ and FeMnZ in minority spin channel as Z changes from Sn, Sb, to Te, in order to get some insight of the large HM gap of FeMnTe. From Table 3, firstly, we notice that the band gaps in minority spin channel of FeMnZ are larger than that of CoMnZ except the case of Z=Sn since CoMnSn prefers an AFM phase. It means that the d–d hybridization between Fe and Mn is stronger than that of Co–Mn, leading to larger band gaps. Secondly, the Fermi level shifts to CBM as the valence electrons of Z increase, while it is rather close to the VBM for the Sn and Sb compounds. For FeMnTe and CoMnTe, the Fermi level reaches nearly the middle of the band gap. Thirdly, the band gaps in minority spin channel get larger as the valence electrons increase for the same row elements of Sn, Sb, and Te. This is not necessarily true for other half-Heusler alloys. For instance, the band gap in minority spin channel of NiCrAs is smaller than that of NiCrSe [24]. Nevertheless, a proper choice of s–p element could increase the HM gaps of half-Heusler alloys by adjusting the Fermi level and band gap of the spin minority, in addition to the prerequisite of strong d–d hybridization of transition metals.

**Table 3**
Calculated $E_{VBM}-E_F$ (corresponding to the negative of HM gap), $E_{CBM}-E_F$ values, and band gap ($E_g$) in the minority-spin channel of CoMnZ and FeMnZ (Z=Sn, Sb, and Te). All the compounds are given for ferromagnetic states.

| Compound | $E_{VBM}-E_F$ (eV) | $E_{CBM}-E_F$ (eV) | $E_g$ (eV) |
|---|---|---|---|
| CoMnSn | 0.26 | 0.99 | 0.73 |
| CoMnSb | −0.17 | 0.73 | 0.90 |
| CoMnTe | −0.42 | 0.71 | 1.13 |
| FeMnSn | −0.04 | 0.48 | 0.52 |
| FeMnSb | −0.20 | 0.77 | 0.97 |
| FeMnTe | −0.61 | 0.63 | 1.24 |

## 4. Conclusions

We have studied the electronic structure and magnetic properties of Te-based half-Heusler alloys, and found that proper choices of anions could maximize the HM gaps of half-Heusler alloys. In particular, we found that CoMnTe and FeMnTe have the largest HM gaps (0.42 and 0.61 eV, respectively) among all the reported Heusler or half-Heusler alloys with the minority spin band gaps of 1.13 and 1.24 eV. The half-metallicity of CoMnTe and FeMnTe can be retained even when their lattice constants change, respectively, from −11.3% to 6.1% and −11.7% to 10.0%. Therefore, the half-Heusler alloys CoMnTe and FeMnTe would be useful for spintronic device applications.

## Acknowledgments

This work is supported by NSFC (Grant no. 11174082). The computer times at National Supercomputing Center in Shenzhen (NSCCSZ) and ScGrid of the Supercomputing Center, Computer Network Information Center of CAS are gratefully acknowledged.

## References

[1] I. Žutić, J. Fabian, S. Das Sarma, Reviews of Modern Physics 76 (2004) 323.
[2] K. Schwarz, Journal of Physics F: Metal Physics 16 (1986) L211.
[3] M.A. Korotin, V.I. Anisimov, D.I. Khomskii, G.A. Sawatzky, Physical Review Letters 80 (1998) 4305.
[4] A. Yanase, K. Siratori, Journal of the Physical Society of Japan 53 (1984) 312.
[5] S. Soeya, J. Hayakawa, H. Takahashi, K. Ito, C. Yamamoto, A. Kida, H. Asano, M. Matsui, Applied Physics Letters 80 (2002) 823.
[6] K.I. Kobayashi, T. Kimura, H. Sawada, K. Terakura, Y. Tokura, Nature 395 (1998) 677.
[7] C.M. Aerts, P. Strange, M. Horne, W.M. Temmerman, Z. Szotek, A. Svane, Physical Review B 69 (2004) 045115.
[8] C.G. Duan, R.F. Sabiryanov, J.J. Liu, W.N. Mei, P.A. Dowben, J.R. Hardy, Physical Review Letters 94 (2005) 237201.
[9] I. Galanakis, P. Mavropoulos, Physical Review B 67 (2003) 104417.
[10] Y.Q. Xu, B.G. Liu, D.G. Pettifor, Physical Review B 66 (2002) 184435.
[11] B.G. Liu, Physical Review B 67 (2003) 172411.
[12] W.H. Xie, Y.Q. Xu, B.G. Liu, D.G. Pettifor, Physical Review Letters 91 (2003) 037204.
[13] S. Ishida, S. Akazawa, Y. Kubo, J. Ishida, Journal of Physics F: Metal Physics 12 (1982) 1111;
S. Ishida, S. Fujii, S. Kashiwagi, S. Asano, Journal of the Physical Society of Japan 64 (1995) 2152.
[14] M. Lezaić, Ph. Mavropoulos, J. Enkovaara, G. Bihlmayer, S. Blügel, Physical Review Letters 97 (2006) 026404.
[15] B. Alling, S. Shallcross, I.A. Abrikosov, Physical Review B 73 (2006) 064418.
[16] M. Sicot, P. Turban, S. Andrieu, A. Tagliaferri, C. De Nadiai, N.B. Brookes, F. Bertran, F. Fortuna, Journal of Magnetism and Magnetic Materials 303 (2006) 54.
[17] C.N. Borca, D. Ristoiu, H.K. Jeong, T. Komesu, A.N. Caruso, J. Pierre, L. Ranno, J.P. Nozières, P.A. Dowben, Journal of Physics: Condensed Matter 19 (2007) 315211.
[18] I. Galanakis, P. Mavropoulos, Journal of Physics: Condensed Matter 19 (2007) 315213.
[19] S. Picozzi, A.J. Freeman, Journal of Physics: Condensed Matter 19 (2007) 315215.
[20] I. Galanakis, E. Şaşıoğlu, K. Özdoğan, Physical Review B 77 (2008) 214417.
[21] P.J. Webster, K.R.A. Ziebeck, Alloys and Compounds of d-Elements with Main Group Elements, Springer, Berlin, Germany (1988) 75–184.
[22] K.R.A. Ziebeck, K.U. Neumann, Magnetic Properties of Metals, Springer, Berlin, Germany (2001) 64–414.
[23] R.A. de Groot, A.M. van der Kraan, K.H.J. Buschow, Journal of Magnetism and Magnetic Materials 61 (1986) 330.
[24] M. Zhang, X. Dai, H. Hu, G. Liu, Y. Cui, Z. Liu, J. Chen, J. Wang, G. Wu, Journal of Physics: Condensed Matter 15 (2003) 7891.
[25] M. Zhang, Z.H. Liu, H.N. Hu, G.D. Liu, Y.T. Cui, G.H. Wu, E. Bruck, F.R. de Boer, Y.X. Li, Journal of Applied Physics 95 (2004) 7219.
[26] Z.Y. Yao, Y.S. Zhang, K.L. Yao, Applied Physics Letters 101 (2012) 062402.
[27] G. Kresse, J. Furthmuller, Physical Review B 54 (1996) 11169.
[28] J.P. Perdew, K. Burke, M. Ernzerhof, Physical Review Letters 77 (1996) 3865.
[29] S.H. Wei, A. Zunger, Physical Review Letters 56 (1986) 528.
[30] T. Graf, C. Felser, S.S.P. Parkin, Progress in Solid State Chemistry 39 (2011) 1.
[31] I. Galanakis, Ph. Mavropoulos, P.H. Dederichs, Journal of Physics D: Applied Physics 39 (2006) 765.
[32] S.Y. Savrasov, Physical Review B 54 (1996) 16470.
[33] M. Lezaic, I. Galanakis, G. Bihlmayer, S. Blugel, Journal of Physics: Condensed Matter 17 (2005) 3121.
[34] T. Block, M.J. Carey, B.A. Gurney, O. Jepsen, Physical Review B 70 (2004) 205114.
[35] J. Rusz, L. Bergqvist, J. Kudrnovský, I. Turek, Physical Review B 73 (2006) 214412.
[36] E. Şaşıoğlu, L.M. Sandratskii, P. Bruno, Physical Review B 72 (2005) 184415.